HHS Public Access

Author manuscript

Hear Res. Author manuscript; available in PMC 2016 September 01.

Published in final edited form as:

Hear Res. 2015 September ; 327: 78–88. doi:10.1016/j.heares.2015.04.014.

Cochlear neuropathy in human presbycusis: confocal analysis of hidden hearing loss in post-mortem tissue

Lucas M. Viana[4], **Jennifer T. O'Malley**[3], **Barbara J. Burgess**[3], **Dianne D. Jones**[3], **Carlos A.C.P. Oliveira**[4], **Felipe Santos**[1,3], **Saumil N. Merchant**[1,2,3], **Leslie D. Liberman**[2,3], and **M. Charles Liberman**[1,2,3]

[1]Department of Otology and Laryngology, Harvard Medical School, Boston MA

[2]Eaton-Peabody Laboratories, Massachusetts Eye & Ear Infirmary, Boston MA

[3]Department of Otolaryngology, Massachusetts Eye and Ear, Boston MA

[4]Faculty of Health Sciences, University of Brasilia, Brasilia, Distrito Federal, Brazil

Abstract

Recent animal work has suggested that cochlear synapses are more vulnerable than hair cells in both noise-induced and age-related hearing loss. This synaptopathy is invisible in conventional histopathological analysis, because cochlear nerve cell bodies in the spiral ganglion survive for years, and synaptic analysis requires special immunostaining or serial-section electron microscopy. Here, we show that the same quadruple-immunostaining protocols that allow synaptic counts, hair cell counts, neuronal counts and differentiation of afferent and efferent fibers in mouse can be applied to human temporal bones, when harvested within 9 hrs post-mortem and prepared as dissected whole mounts of the sensory epithelium and osseous spiral lamina. Quantitative analysis of five "normal" ears, aged 54 to 89 yrs, without any history of otologic disease, suggests that cochlear synaptopathy and the degeneration of cochlear nerve peripheral axons, despite a near-normal hair cell population, may be an important component of human presbycusis. Although primary cochlear nerve degeneration is not expected to affect audiometric thresholds, it may be key to problems with hearing in noise that are characteristic of declining hearing abilities in the aging ear.

Keywords

Presbycusis; human temporal bone; auditory neuropathy; cochlear synaptopathy

Correspondence to: M. Charles Liberman Ph.D., Eaton-Peabody Laboratories, Massachusetts Eye and Ear Infirmary, 243 Charles St., Boston, MA 02114-3096, USA., Tel: 617-573-3745, Fax: 617-720-4408, Charles_Liberman@meei.harvard.edu.

Contributions

CACPO and DDJ arranged for temporal bone removal at autopsy. BJB and FS assisted in histological preparation. JTO and LDL developed and carried out the immunostaining protocols. LMV, JTO and LDL assisted in data acquisition and analysis. SNM and MCL conceived of the experiments. MCL performed data acquisition and analysis and wrote the manuscript.

Introduction

The idea that cochlear neural degeneration is a contributing factor in age-related hearing loss is an old one, indeed neural presbycusis is one of the four “types” of presbycusis originally proposed by Schuknecht (Schuknecht, 1993) based on his analysis of sectioned human temporal bones. However, until recently, the prevailing view has been that most of the degeneration of cochlear nerve fibers only occurs secondarily to, and because of, the loss of sensory cells (Bohne et al., 2000). Similarly, it has been widely assumed that primary neural degeneration, i.e. significant loss of cochlear nerve fibers in the absence of significant hair cell loss, is largely restricted to relatively rare types of genetic hearing loss such as Mohr-Tranebjaerg syndrome (Bahmad et al., 2007), Freidrich’s ataxia (Spoendlin, 1974), Usher’s syndrome (Nadol, 1988b), or to special classes of acquired sensorineural hearing loss such as Meniere’s disease (Nadol, 1988b).

Recent work in animal models has shown, in both noise-induced and age-related types of acquired sensorineural hearing loss, that there can be significant loss of cochlear nerve terminals well before there is significant loss of either inner or outer hair cells (Kujawa et al., 2009; Sergeyenko et al., 2013). For example, even after noise exposures causing only transient threshold elevation and no hair cell loss, there can be immediate and irreversible loss of 40–50% of the cochlear nerve synapses on inner hair cells (Kujawa et al., 2009). Similarly, in aging mice, there is a 25–30% loss of cochlear nerve synapses by middle age, well before there is any loss of hair cells or significant threshold elevation (Sergeyenko et al., 2013). Although the disappearance of these cochlear nerve synapses occurs very rapidly (within hours) after noise, the death of the cell bodies in the spiral ganglion is extremely slow (over 1–2 years in the mouse).

The delayed death of spiral ganglion cells is part of the reason why this type of noise-induced neuropathy remained undiscovered for so long. Another part of the reason is that the peripheral terminals of cochlear nerve fibers are unmyelinated and thus invisible in standard histopathologic preparation of cochlear tissue. To see, and count, the synapses and unmyelinated peripheral terminals of cochlear nerve fibers requires immunostaining of pre- and post-synaptic elements (Kujawa et al., 2009). Fortunately, the cochlear synapses are ribbon synapses, and excellent antibodies are available for a prominent protein in these pre-synaptic ribbons (Khimich et al., 2005; Schmitz et al., 2000). A number of neuronal markers, e.g. anti-neurofilament, are also available to help see both myelinated and unmyelinated nerve fibers in the inner ear (Berglund et al., 1991).

The other reason why noise-induced neuropathy remained undiscovered is that diffuse degeneration of the cochlear nerve in the absence of hair cell loss has minimal effects on pure-tone thresholds. This important fact has been known since the 1950’s, when Schuknecht and others demonstrated that partial section of the auditory nerve, destroying more than 50% of cochlear nerve fibers throughout the cochlear spiral, had no measurable effect on the audiograms of behaviorally trained cats (Schuknecht et al., 1955). The phenomenon of primary cochlear neural degeneration has been called “hidden hearing loss”, because the pathology hides behind a normal audiogram (Schaette et al., 2011). Despite, the lack of effect on pure-tone thresholds, it is likely that primary neural degeneration has

profound effects on more complex auditory tasks, such as understanding speech in a noisy environment, and such difficulties are a classic complaint of patients with sensorineural hearing loss of many types (Frisina et al., 1997).

Inspired by the discovery of noise-induced and age-related primary neural degeneration in animal models, we re-examined the spiral ganglion in an age-graded series of human temporal bones, concentrating only on those cases with no explicit otologic disease and no significant loss of inner or outer hair cells (Makary et al., 2011). Indeed, we found a steady decline in spiral ganglion counts from birth to death, despite the lack of hair cell loss, corresponding, on average to a loss of more than 30% of cochlear neurons over a lifetime. However, given the long delay between the loss of synaptic connection with the inner hair cell and the death of the cell body, we hypothesized that the true degree of cochlear synaptopathy was greatly underestimated by merely counting the cell bodies in the spiral ganglion.

To test this hypothesis, we set out to apply, to human temporal bones, the immunostaining approaches that had proven so successful in animal studies of cochlear neuropathy. Here, we show that these triple- and quadruple-immunostains can often reveal a wealth of quantitative information about the patterns of afferent and efferent innervation in human post-mortem material. We also show evidence suggesting that cochlear synaptopathy, in the absence of hair cell loss, may be a more important factor in human presbycusis than previously recognized.

Materials and Methods

Tissue preparation and image acquisition

Human temporal bones were extracted at autopsy using standard techniques, as described elsewhere (Schuknecht, 1993). This temporal-bone study has been approved by the Human Studies Commitee of the Massachusetts Eye and Ear Infirmary. Post-mortem times varied between 9 and 39 hrs. Several hours after removal of the bone plug containing the inner ear, the round and oval windows were opened and a fixative solution (10% formalin) was perfused through the cochlear scalae. The ear remained in this fixative solution for 5–9 days at 4° C. After post-fixation, the petrous bone was drilled down, leaving only a thin capsule around in the cochlear scalae. Then, the ear was decalcified in 0.12M EDTA for 20–62 days at room temperature. When the bone was thoroughly decalcified, the organ of Corti and osseous spiral lamina was manually dissected into 8–9 pieces.

Immunostaining began with a blocking buffer (PBS with 5% normal horse serum and 0.3 −1% Triton X-100) for 1 h at room temperature and followed by overnight incubation at 37 °C with some combination of the following primary antibodies: 1) mouse (IgG1) anti-CtBP2 (C-terminal Binding Protein; BD Biosciences #612044) at 1:200 to quantify pre-synaptic ribbons: 2) chicken anti-neurofilament (Chemicon #AB5539) at 1:1000 to quantify nerve axons, 3) rabbit anti-Myosin VIIa (Proteus Biosciences #25–6790) at 1:200 to count hair cells and 4) goat anti-ChAT (choline acetyltransferase; Millipore #AB144P) at 1:100 to count efferent axons from the olivocochlear bundle. Primary incubations were followed by 2 sequential 60-min incubations at 37°C in species-appropriate secondary antibodies (coupled

to Alexafluor dyes) with 0.3 – 1% TritonX. After immunostaining, all pieces from each cochlea were slide-mounted in Vectashield, coverslipped, and the coverslip was sealed with nail polish.

Data Analysis

A cochlear frequency map was prepared for each case using a custom plug-in to ImageJ with which the user traces an arc along the union of the heads of the pillar cells on a low-power micrograph of each dissected piece of the cochlear spiral. After computing the total length, the plug-in computes and displays the locations of each half-octave frequency point along the spiral, using the cochlear frequency map for human (Schuknecht, 1993).

Images were acquired on a Leica SP5 confocal microscope. To count synaptic ribbons, hair cells and cochlear nerve fibers, image stacks were acquired at 0.25 mm z-spacing using a 63x glycerol-immersion objective (N.A. = 1.3). The z-stacks were then ported to a workstation running Amira® software. Ribbons were counted using the connected components feature that automatically finds (and displays in 3D) all the enclosed volumes within which pixel intensity in the appropriate confocal channel is greater than a user-defined criterion. Peripheral axons of cochlear nerve fibers and olivocochlear efferents were counted manually in virtual slices taken orthogonal to the plane of the osseous spiral lamina. In each z-stack, the position of that virtual slice was adjusted in Amira to find the location that maximized the number of immunostained profiles in the appropriate confocal channel. Hair cells were counted manually from a maximum projection of the portion of the z-stack including the cuticular plates, because the myosin VIIa immunoreactivity was strongest in that region and the cellular organization was least disrupted.

Results

A. Selection of material, overall success rate and qualitative observations

The aim of the present study was to evaluate the age-related changes in cochlear innervation in “normal” ears, i.e. those without significant hair cell loss. To that end, post-mortem specimens obtained by the Otopathology Laboratory at the Massachusetts Eye and Ear from individuals with no mention of otologic disease in their medical history were selected for processing by cochlear dissection and immunostaining. Of the 19 temporal bones processed in this way, eight had post-mortem times less than or equal to 11.5 hours, and, in all of these cases, the immunostaining protocols were at least partially successful. Of the remaining 11, with postmortem times ranging from 12–60 hrs, usable images were obtained from only one case, with a post-mortem time of 21 hrs.

In five of the eight well-stained cases, the five most recent cases, the entire cochlear spiral was successfully removed, and the organ of Corti was analyzable from base to apex. Postmortem times in these cases were ≤ 11.5 hrs. It is on these five complete cases (from 4 individuals) that the quantitative analysis in this report is based.

B. Counting hair cells

Myosin VIIa is one of several unconventional myosins expressed in hair cells, and it is used widely as a hair cell marker in animal studies (Hasson et al., 1997). As in animal studies, the staining in our human temporal bones tended to be stronger in the apical half of the cochlea than the basal half of the cochlea, and stronger in the outer hair cells (OHCs) than the inner hair cells (IHCs). The anti-myosin VIIa immunostaining was very useful in counting hair cells. As shown in Figure 1A, the cuticular plates of the IHCs and OHCs stain brightly for myosin VIIa and it is easy to create a cytocochleogram of each dissected ear from images such as these, sampled at octave (Fig. 1B,D) or half-octave (Fig. 1C,E) intervals along the cochlear spiral. These four cytocochleograms show that, for each of the completely reconstructed subjects in this study, the loss of hair cells, especially the IHCs, was minimal outside of the hook region of the cochlea: the fifth case analyzed was the left ear of the 67 yr old female, which was very similar to the right ear shown in panel C. Note that the frequency axis for these cytocochleograms spans the entire human frequency range (0.12 – 19 kHz) at least as defined by Schuknecht's cochlear frequency map (Schuknecht, 1993).

C. Differentiating afferent from efferent fibers

Immunostaining for neurofilament protein can be excellent way to visualize all of the afferent and efferent fibers in the inner ear (Maison et al., 2006), depending on which molecular weight neurofilaments are targeted. Our anti-neurofilament label was extremely strong in all the cases, at all cochlear regions. In low-power views at different cochlear locations, the radially directed bundles of peripheral axons of the spiral ganglion cells are easily visible in the osseous spiral lamina (OSL, Fig. 2). In the organ of Corti, the neurofilament label clearly reveals the three spiraling rows of outer spiral fibers, the peripheral projections of type-II spiral ganglion cells innervating the outer hair cells (OHCs) (Kiang et al., 1982).

Double-staining for a cholinergic marker can highlight the efferent fibers of the olivocochlear bundle (Schrott-Fischer et al., 2007): here we used antibodies to choline acetyltransferase (ChAT), an enzyme in the biosynthetic pathway for the cholinergic neurotransmitter. As expected, the olivocochlear fibers take a predominately spiral course through the OSL, indeed all the spiraling fiber bundles in the OSL are immunopositive for ChAT (Fig. 2). In the low-power views, the ChAT label also highlights the terminal processes of medial olivocochlear neurons crossing the tunnel of Corti to the OHCs. The peripheral terminals of these medial olivocochlear neurons on the bases of the OHCs are also clearly visible in the high-power view of the triple-stained organ of Corti shown in Figure 3, both as seen from the endolymphatic surface (Fig. 3A; xy view) and as re-projected from the "side" (Fig. 3B; zx view). Olivocochlear terminals are also present in the inner hair cell (IHC) area where they are presumably synapsing with the dendrites of type-I sensory neurons and within the tunnel of Corti where they are likely synapsing with projections of the type-II fibers innervating OHCs (Liberman, 1980a) (Figs 3A,B)

In one case, the neurofilament immunostain revealed a long spiraling process well outside the third row OHCs (green arrow in Fig. 2A). Presumably this corresponds to the fibers in the Hensen cell area previously identified in the electron microscope in the guinea pig

cochlea (Burgess et al., 1997). Consistent with data from surgically de-efferented guinea pigs (Fechner et al., 1998), the lack of ChAT immunostaining here (Fig. 2A) suggests that this fiber is part of the type-II afferent system rather than a branch of an olivocochlear efferent fiber. This type of spiraling Hensen cell projection was only seen in one (apical) cochlear piece from one case, thus the phenomenon does not appear to be a regular aspect of the cochlear innervation in humans.

D. Counting IHC synapses with type-I ganglion cells

In experimental animals, where it has been most exhaustively studied, each type-I spiral ganglion cell sends a single myelinated peripheral axon to the organ of Corti where it loses its myelin and contacts a single IHC via a single terminal dendrite (Liberman, 1980b; Spoendlin, 1969). At the IHC contact there is a single active zone characterized, in electron micrographs, by pre- and post-synaptic membrane thickenings and an electron-dense pre-synaptic ribbon around which the synaptic vesicles are tethered (Liberman, 1980b). Thus, immunostaining for synaptic ribbons produces a set of puncta studding the basolateral surface of the IHCs, which serves as an excellent proxy for the set of synaptic contacts of the type I neurons (Liberman et al., 2011).

In the present study, CtBP2-positive puncta were always visible in the IHC and OHC areas wherever hair cells were present, and the association between myosin-VIIa staining and clusters of CtBP2-positive puncta was very clear, as shown for the OHC and IHC areas in Figures 4 and 5, respectively. Note for example, in the high-frequency IHC region, where there is spotty loss of IHCs, that the CtBP2-positive puncta are only present where the IHCs are present (Fig. 5E). The locations of the pre-synaptic ribbons around the basolateral surface of the hair cells is well seen by re-projecting the confocal z stack as a maximum projection into the zx plane, as shown in Figures 4B, 5B,D,F. Although most of the pre-synaptic ribbons are seen near the basal pole of the hair cells, where the dendrites of the cochlear nerve fibers terminate (green arrows in Fig. 5), some “orphan” ribbons appear to be located far from the neuronal terminals (Fig. 4B; red arrows in Fig. 5B,D,F).

The association between ribbons and terminals in the IHC area was analyzed in more detail by replotting the voxel space immediately around each CtBP2-positive punctum and evaluating the entire set from each z-stack. A selected sample of these thumbnail images is shown in Figure 6A. As shown more systematically in Figure 6B, the fraction of ribbons closely paired with nerve terminals varied from case to case and from cochlear region to cochlear region. In general, the smallest numbers of orphan ribbons were seen in the youngest ear (54 yrs), where the values ranged between 20 and 40% of the sample (Fig. 6B). Even in well-fixed ears from experimental animals, the percentage of ribbons without closely paired neurofilament-positive immuno-label is around 25% (Lin et al., 2011). Given that ultrastructural studies suggest a close pairing between ribbons and terminals (Nadol, 1983), the relatively high percentage of orphan ribbons may reflect the fact that neurofilament bundles may not always invade the very tip of the cochlear nerve terminal. In the older ears from the present study, the percentage of orphan ribbons was highest in the apical and basal extremes of the cochlea (Fig. 6B). Some of the orphan CtBP2-positive

puncta are located intracellularly, i.e. too far from the plasma membrane to be associated with synapses. This may reflect pathological change in the older ears.

Counts of synaptic ribbons per IHC suggest an age-related gradient, as shown in Figure 7B. In the youngest ear of the group, the counts varied between 11.1 and 13.3 synapses per IHC, outside of the basalmost location, whereas in the oldest ear the counts were never higher than 7.6 (at 0.25 kHz) and fell as low as 2.0 synapses per IHC, even as far apicalwards as the 2 kHz region.

E. Counting peripheral axons of type-I ganglion cells

Prior serial-section ultrastructural work in the human cochlea shows that one cochlear nerve terminal can make multiple *en passant* synapses with a single hair cell or two adjacent hair cells (Nadol, 1983). Thus, the ribbon counts could overestimate the numbers of connected spiral ganglion cells remaining in each case. To gain some insight into this issue, we estimated the number of peripheral axons of type-I neurons in the OSL. As shown in Figure 8, the confocal z-stacks obtained in a plane parallel to the OSL can be digitally re-sliced in the xz plane to view virtual cross-sections in which immunostained neural elements can be counted in the channel corresponding to the anti-neurofilament immunolabel. Cochlear neuroanatomy suggests that the bulk of these radially directed OSL neurons are peripheral axons of type I's: firstly, the type I afferents outnumber type-II's by 20:1 (Spoendlin, 1969), and, secondly, spiral ganglion cells (∼40,000 (Makary et al., 2011)) outnumber olivocochlear neurons (∼3000 (Moore et al., 1999)) by more than 10:1. Furthermore, the unmyelinated peripheral axons of type-II neurons are extremely fine (Brown, 1987) and may tend to be undercounted in this material.

To be more quantitative, we removed olivocochlear neurons from the OSL counts using two complementary strategies. First, we compared counts of fibers in the OSL to counts of fibers crossing the middle of the tunnel of Corti, where medial olivocochlear fibers cross to the OHCs (Spoendlin et al., 1963). Based on that comparison, we estimated that the percentage of neurofilament-positive fibers in the OSL that were medial olivocochlear in origin ranged from 10 – 20% throughout much of the cochlear spiral, except in the oldest ear where the total number of OSL neurons was extremely low (Fig. 7A). Secondly, in two of the five cases (the most recent ones processed), we added an anti-ChAT immunolabel in the fourth confocal laser channel to selectively label the olivocochlear neurons. Comparing the numbers of ChAT- and neurofilament-positive fibers in these virtual cross-sections suggested, again, that olivocochlear neurons comprise only ∼13% of the radially directed OSL fibers throughout most of the cochlear spiral (Fig. 9).

Corrected in this way, the estimated numbers of type-I peripheral axons per IHC peaks in the middle of the cochlea at values close to 14 in the youngest ear analyzed (Fig. 7A), which is similar to the peak number of ribbons per IHC in the same ear (Fig. 7B). As shown in Figure 7C, the ratio of ribbon counts to Type-I axonal counts was close to 1 in cochlear regions between 0.25 kHz and 2 kHz, excluding the oldest ear, in which there were very few fibers remaining in the OSL. In the oldest ear, and in the apical and basal ends of all the ears, the ribbons outnumber peripheral axons by as much as 5 to 1 (Fig. 7C).

Discussion

A. Spiral ganglion counts as a metric of cochlear neuropathy

Based on extensive analysis of human temporal bones prepared as semi-serial celloidin sections stained with hematoxylin and eosin, Schuknecht devised a classification scheme for human presbycusis suggesting there are four basic types. Because his analysis was fundamentally histopathological, the organizational scheme was fundamentally based on the tissue types showing the most dramatic light-microscopic histopathology, i.e. sensory cells, cochlear neurons, or the stria vascularis (Schuknecht, 1993). Because there were also numerous cases of presbycusis in his temporal bone collection that showed minimal histopathology in any of these three tissues, he proposed a fourth type, cochlear conductive, suggesting that there could be changes in the thickness/stiffness of the basilar membrane and/or spiral ligament that would affect mechanical propagation of the cochlear traveling wave. However, a more recent quantitative analysis of the basilar membrane in an age-graded series of temporal bones found no significant differences in thickness between cases with normal audiograms and those with age-related threshold elevation (Bhatt et al., 2001), thus the idea of cochlear conductive changes remains highly speculative as a significant contributing factor to age-related hearing loss.

The importance of hair cell loss, neuronal loss and strial degeneration to presbycusis is undeniable, but the relative contribution and prevalence of each is less well understood. Loss of hair cells is easy to quantify in a variety of histological preparations of the cochlea. Thus, hair cell loss has been amply documented in human studies of the aging ear (e.g. (Soucek et al., 1986)) and obviously contributes to threshold elevation in any affected cochlear regions. Although strial degeneration is harder to quantify, it too has been amply documented in animal and human studies (Ohlemiller et al., 2006; Pauler et al., 1988), and any resultant decrease in the endolymphatic potential will also contribute to threshold elevation in affected regions. Indeed, experiments in the aging gerbil show that, in this mammalian species, strial pathology is evident before hair cell loss, and the elevation of cochlear thresholds is well correlated with the age-related decrease in the endolymphatic potential (Schmiedt et al., 1992).

Neural loss in the presbycusic ear has been more difficult to accurately measure. Animal studies of acquired sensorineural hearing loss show a significant delay between the death of hair cells and the disappearance of spiral ganglion cells. In noise damage, for example, the loss of hair cells occurs within days, while the disappearance of cochlear nerve peripheral axons is delayed by several weeks, and loss of spiral ganglion cell bodies and central axons continues for months, if not years (Liberman et al., 1978). Since most human histopathology is done via light-microscopic evaluation of serial sections, and since peripheral axons in the OSL are difficult to quantify in cochlear sections, most human studies have relied on spiral ganglion cell counts in the assessment of cochlear neural degeneration (Miura et al., 2002; Otte et al., 1978; Seyyedi et al., 2011). Since the ganglion cell death is significantly delayed with respect to the loss of synaptic connections to hair cells, these cell counts must significantly underestimate the functional cochlear neuropathy. The delay between loss of peripheral axons and death of the spiral ganglion cell may be particularly elongated in the

human cochlea. A study comparing counts of peripheral and central axons in cochleas from an age-graded series of 45 temporal bones concludes that, whereas counts are similar in the two locations in young ears, counts in old ears are always lower for peripheral axons than for central axons, suggesting that cell bodies without peripheral axons can survive in humans for decades (Felix et al., 2002).

The delay between hair cell loss and spiral ganglion cell loss in acquired sensorineural hearing loss has also led to the idea that hair cells are typically the primary target, and that neuronal degeneration occurs only secondarily to, and as a result of, the loss of hair cells and the neurotrophic support that they provide. Recent work on noise damage in mice and guinea pigs has challenged this view, showing that exposures causing only transient threshold elevation and no hair cell loss nevertheless cause significant cochlear neuropathy (Kujawa et al., 2009). This primary cochlear neuropathy is visible immediately post-exposure as a loss of cochlear-nerve synapses on IHC, while the loss of spiral ganglion cells is delayed by as much as 2 years. Similarly, in aging mice, the loss of IHC synapses occurs well before there is significant loss of hair cells (Sergeyenko et al., 2013). It is also now clear that loss of IHCs, *per se*, need not cause degeneration of cochlear nerve fibers (Zilberstein et al., 2012). Rather it appears that supporting cells in the IHC area are the most critical sources of neurotrophic support, and that the neuronal death in regions of hair cell loss after noise and ototoxic drugs is likely the result of direct neuronal damage in the acute phases of the cochlear insult (Liberman et al., 1982; Robertson, 1983).

B. Counting peripheral axons in human post-mortem material

The idea that primary cochlear neurodegeneration may be more important in noise-induced and age-related hearing loss than previously appreciated (Kujawa et al., 2009; Sergeyenko et al., 2013) inspired us to apply new histological approaches based on immunostaining and confocal microscopy of microdissected whole mounts of the organ of Corti to the study of human cochlear pathology. Work in animal models showed that this approach enabled quantitative light-microscopic analysis of the unmyelinated terminals of cochlear nerve fibers and their hair cell synapses that, prior to the development of robust immuno-markers of cochlear pre- and post-synaptic elements, could only be studied in the electron microscope via serial section analysis, an extremely labor-intensive process (Liberman, 1980b; Nadol, 1983; Stamataki et al., 2006).

As we show here, the analysis of immunostained whole mounts enables rapid counting of cochlear-nerve peripheral axons (Fig. 8). Although imaged in a plane parallel to the fibers, a confocal image stack through the OSL, which can be acquired in 1–2 minutes, can be digitally sectioned to produce a cross-sectional view in which the individual neurofilament-stained elements can be quickly and accurately counted (Fig. 7B). Others have used light-microscopic analysis of cochlear whole mounts to count peripheral axons in human ears, both with and without explicit otological disease (Felder et al., 1995; Spoendlin et al., 1989). In prior studies, cochleas were plastic-embedded, so that pieces of the cochlear spiral could be viewed as “surface preparations” prior to re-sectioning in a plane perpendicular to the OSL to count peripheral axons, as in the xz projections from Figure 8. In one study using this “block surface” method, Spoendlin and colleagues counted peripheral axons, at 10

equally spaced cochlear locations, from 6 ears with “normal hearing”, including both ears from a 7 yr old and one ear each from individuals aged 40, 49, 51 and 60 yrs (Spoendlin et al., 1990). In Figure 10B, we have converted their counts, expressed as nerve fibers per mm of organ of Corti, to counts of nerve fibers per IHC, using the mean value of 94.3 IHCs/mm extracted from our myosin VIIa immunostaining (e.g. Figure 1A). Two salient points emerge from this comparison: 1) the fiber counts in the youngest ear from the present study (age 54) are similar to the mean counts for ears aged 7 yrs to 61 yrs in the prior study (average of two 7-yr old ears is shown in Fig. 10B for comparison), and 2) across the two studies, there appears to be little change in peripheral axon counts among “normal hearing” people aged 7 to roughly 60 yrs of age.

We can also use the mean values for peripheral axons per IHC, sampled at 8 log-spaced intervals along the cochlear spiral (Fig. 7A), to estimate the total number of Type-I peripheral axons in each ear. Using a mean cochlear length of 32 mm (Schuknecht, 1993), and the value of 94.3 IHCs/mm cited above, gives rise to an estimated 3017 IHCs per human cochlea. When divided into 8 equal segments, this yields 377 IHCs/segment as the multiplier for the mean values of peripheral axons / IHC extracted from the confocal z-stacks (Fig. 7). When summed across all segments, the estimated peripheral axons counts can be compared to spiral ganglion cell counts obtained from an age-graded series of serially sectioned human temporal bones from a prior study (Makary et al., 2011). As shown in Figure 10A, the comparison suggests that, in the youngest ear (age 54 yrs), the vast majority of spiral ganglion cells still have peripheral axons. In contrast, the disparity between the two measures in three of the older ears suggests that spiral ganglion cells survive in much greater numbers than peripheral axons, and thus that ganglion cell counts greatly underestimate the functional neuropathy in elderly people, even those without explicit otologic disease or significant hair cell loss.

C. Counting IHC synapses in human post-mortem material

Although peripheral axon counts are likely a more functionally important metric than spiral ganglion counts, when considering hearing abilities without a cochlear implant, it is most important to understand how many of the surviving peripheral axons are still synaptically connected to hair cells. Since 95% of cochlear nerve fibers in mammalian ears are type-I cells innervating IHCs (Spoendlin, 1972), it is the synaptology in the IHC area that is the most critical to evaluating the functional capacity of the cochlear nerve in human presbycusis.

In work with mice and guinea pigs, immunostaining and counting the pre-synaptic ribbons in the IHC area is an excellent proxy for the assessment of cochlear nerve synapses. In the normal mouse ear, counts of CtBP2-positive puncta per IHC are identical to counts of cochlear nerve synapses per IHC seen in serial section electron microscopy (Kujawa et al., 2009; Stamataki et al., 2006), because each cochlear nerve synapse contains a pre-synaptic ribbon and almost all ribbons are paired with post-synaptic elements (Liberman, 1980b; Nadol, 1983). Although the number of orphan ribbons, i.e. those unpaired with cochlear nerve terminals, is slightly increased in noise-exposed and aging mouse cochleas, the percentages remains very small (< 5% (Liberman et al., 2015; Sergeyenko et al., 2013)). In

normal ears, there are sometimes multiple ribbons present at a single synaptic contact (Merchan-Perez et al., 1996; Nadol, 1983). However, doublets and triplets are likely not resolved in the confocal microscope as the separation distance (i.e. 50 nm (Merchan-Perez et al., 1996)) is significantly smaller than can be resolved in the light microscope.

Here we show that, in mid-cochlear locations in most ears, there is a close correspondence between the number of ribbons and the number of peripheral axons in the OSL (Fig. 7C). In apical and basal regions, there were more ribbons than fibers, and, in the oldest ear, the ribbon counts outnumbered the neuronal counts throughout most of the cochlear spiral. In the cochlear apex, even in normal ears, cochlear nerve fibers can branch and/or form multiple en passant synaptic swellings, especially in human cochleas (Nadol, 1983). This may account for some of the increased counts for ribbons *re* peripheral axons. However, the increased ratios in the basal cochlear regions, and especially in the oldest and arguably most pathological specimen, suggests there may be a profusion of orphan ribbons in regions of cochlear pathology. The location of many orphan puncta far from the plasma membrane is consistent with the idea that they reflect a type of pathological change.

In cochlear regions where ribbon counts and neuronal counts are comparable, the confocal-derived estimates of synaptic terminals per IHC agree with values extracted from serial section electron microscopic analysis of human IHCs (Nadol, 1983). As is also summarized in Figure 10B, these ultrastructural counts from a “normal hearing” 64 yr old, ranging from 6.5 to 12.5 terminals per IHC depending on cochlear location, are remarkably similar to the confocal-derived estimates for our “normal hearing” individuals aged 54 – 67 yrs.

Taken together, these light- and electron-microscopic studies suggest that the great majority of peripheral axons in the OSL in aging human ears remain in synaptic contact with IHCs, and thus that whatever delay there is between the loss of the peripheral synapse and the loss of the peripheral axon, it is short enough that the counts of peripheral axons should provide an accurate estimate of the numbers of potentially functional cochlear sensory fibers in the ear. On the other hand, it is also abundantly clear that many spiral ganglion cells survive, along with their central axons, for many years, if not decades, after the degeneration of their peripheral axons. Such monopolar ganglion cells are of no obvious relevance to hearing, absent a cochlear implant. Thus, the evaluation of spiral ganglion cell death greatly underestimates the degree of cochlear neuropathy in a human temporal bone. Given that neurofilament immunolabeling was robust in every temporal bone preparation we examined, this approach to the quantification of peripheral axons should be widely applicable to study of neural presbycusis in human post-mortem material. The immunohistochemical approach we have applied here has added benefits over other whole-mount techniques such as the block surface technique, which use conventional nerve stains such as osmium or silver. Immunohistochemical approaches allow for staining of multiple features; for example, as applied here, a quadruple stain augmented the labeling of cochlear nerve axons with overlays for 1) cholinergic markers to definitively exclude efferent fibers from the axonal counts, 2) hair cell markers to simplify the task of counting sensory cell loss, and 3) ribbon markers to further clarify the condition of IHC synapses.

D. The importance of age-related primary cochlear neuropathy in human presbycusis

Data from this, and prior, studies focused on the cochlear innervation in aging human ears strongly suggest that loss of cochlear nerve connections to the hair cells can occur well before the loss of hair cells, and thus that primary neural degeneration could be an important aspect of presbycusis, especially in individuals older than their mid-fifties. The present study is preliminary in nature, in that the sample of human temporal bones is small. It is interesting that prior studies of human ears with minimal hair cell loss, using the block surface method designed to accurately count cochlear nerve peripheral axons, also concluded that neuronal counts were well maintained until around 60 yrs of age, after which time many ears began to show significant loss of peripheral axons, without a concomitant loss of central axons (Felder et al., 1995; Spoendlin et al., 1989; Spoendlin et al., 1990).

In thinking about the functional consequences of this type of primary neural degeneration it is important to remember that cochlear nerve loss, *per se*, has no significant effect on audiometric thresholds until that loss exceeds 90% (Lobarinas et al., 2013; Schuknecht et al., 1955). It has long been hypothesized that the functional manifestation of this type of neuropathy should be difficulties in speech comprehension, especially in a noisy environment. Indeed, one of the prior studies of human temporal bones by the block-surface method included measures of speech discrimination and noted that those aging ears with 50% or more loss of peripheral axons began to show significant deficits in word recognition tests, even in quiet (Felder et al., 1995).

The slow death of the spiral ganglion cell body and its central axon provides a long therapeutic window during which treatments designed to elicit neurite extension from surviving spiral ganglion cells could theoretically reconnect neurons and hair cells and rescue the hearing impairment associated with noise-induced or age-related cochlear neural degeneration. Indeed, recent experiments in transgenic mice overexpressing the most important cochlear neurotrophic factor, NT-3, suggest that such rescue from noise-induced synaptopathy can be achieved (Wan et al., 2014).

Acknowledgments

Research supported by grants from the NIDCD: R01 DC 0188, P30 DC 05209 and U24 DC 011943

References Cited

Bahmad F Jr, Merchant SN, Nadol JB Jr, Tranebjaerg L. Otopathology in Mohr-Tranebjaerg syndrome. Laryngoscope. 2007; 117:1202–1208. [PubMed: 17471106]

Berglund AM, Ryugo DK. Neurofilament antibodies and spiral ganglion neurons of the mammalian cochlea. J Comp Neurol. 1991; 306:393–408. [PubMed: 1865000]

Bhatt KA, Liberman MC, Nadol JB Jr. Morphometric analysis of age-related changes in the human basilar membrane. Ann Otol Rhinol Laryngol. 2001; 110:1147–1153. [PubMed: 11768706]

Bohne BA, Harding GW. Degeneration in the cochlea after noise damage: primary versus secondary events. Am J Otol. 2000; 21:505–509. [PubMed: 10912695]

Brown MC. Morphology of labeled afferent fibers in the guinea pig cochlea. J Comp Neurol. 1987; 260:591–604. [PubMed: 3611412]

Burgess BJ, Adams JC, Nadol JB Jr. Morphologic evidence for innervation of Deiters' and Hensen's cells in the guinea pig. Hear Res. 1997; 108:74–82. [PubMed: 9213124]

Fechner FP, Burgess BJ, Adams JC, Liberman MC, Nadol JB Jr. Dense innervation of Deiters' and Hensen's cells persists after chronic deefferentation of guinea pig cochleas. J Comp Neurol. 1998; 400:299–309. [PubMed: 9779936]

Felder E, Schrott-Fischer A. Quantitative evaluation of myelinated nerve fibres and hair cells in cochleae of humans with age-related high-tone hearing loss. Hear Res. 1995; 91:19–32. [PubMed: 8647720]

Felix H, Pollak A, Gleeson M, Johnsson LG. Degeneration pattern of human first-order cochlear neurons. Adv Otorhinolaryngol. 2002; 59:116–123. [PubMed: 11885652]

Frisina DR, Frisina RD. Speech recognition in noise and presbycusis: relations to possible neural mechanisms. Hear Res. 1997; 106:95–104. [PubMed: 9112109]

Hasson T, Gillespie PG, Garcia JA, MacDonald RB, Zhao Y, Yee AG, Mooseker MS, Corey DP. Unconventional myosins in inner-ear sensory epithelia. The Journal of cell biology. 1997; 137:1287–1307. [PubMed: 9182663]

Khimich D, Nouvian R, Pujol R, Tom Dieck S, Egner A, Gundelfinger ED, Moser T. Hair cell synaptic ribbons are essential for synchronous auditory signalling. Nature. 2005; 434:889–894. [PubMed: 15829963]

Kiang NY, Rho JM, Northrop CC, Liberman MC, Ryugo DK. Hair-cell innervation by spiral ganglion cells in adult cats. Science. 1982; 217:175–177. [PubMed: 7089553]

Kujawa SG, Liberman MC. Adding insult to injury: cochlear nerve degeneration after "temporary" noise-induced hearing loss. J Neurosci. 2009; 29:14077–14085. [PubMed: 19906956]

Liberman LD, Wang H, Liberman MC. Opposing gradients of ribbon size and AMPA receptor expression underlie sensitivity differences among cochlear-nerve/hair-cell synapses. The Journal of neuroscience : the official journal of the Society for Neuroscience. 2011; 31:801–808. [PubMed: 21248103]

Liberman LD, Suzuki J, Liberman MC. Dynamics of cochlear synaptopathy after noise exposure. Journal of the Association for Research in Otolaryngology In Press. 2015

Liberman MC. Efferent synapses in the inner hair cell area of the cat cochlea: An electron microscopic study of serial sections. Hear Res. 1980a; 3:189–204. [PubMed: 7440423]

Liberman MC. Morphological differences among radial afferent fibers in the cat cochlea: An electron-microscopic study of serial sections. Hear Res. 1980b; 3:45–63. [PubMed: 7400048]

Liberman MC, Kiang NY. Acoustic trauma in cats. Cochlear pathology and auditory-nerve activity. Acta Otolaryngol Suppl. 1978; 358:1–63. [PubMed: 281107]

Liberman, MC.; Mulroy, MJ. Acute and chronic effects of acoustic trauma: Cochlear pathology and auditory nerve pathophysiology. In: Hamernik, RP.; Henderson, D.; Salvi, R., editors. New Perspectives on Noise-Induced Hearing Loss. 1982. p. 105-136.

Lin HW, Furman AC, Kujawa SG, Liberman MC. Primary neural degeneration in the Guinea pig cochlea after reversible noise-induced threshold shift. J Assoc Res Otolaryngol. 2011; 12:605–616. [PubMed: 21688060]

Lobarinas E, Salvi R, Ding D. Insensitivity of the audiogram to carboplatin induced inner hair cell loss in chinchillas. Hearing research. 2013

Maison SF, Rosahl TW, Homanics GE, Liberman MC. Functional role of GABAergic innervation of the cochlea: phenotypic analysis of mice lacking GABA(A) receptor subunits alpha 1, alpha 2, alpha 5, alpha 6, beta 2, beta 3, or delta. J Neurosci. 2006; 26:10315–10326. [PubMed: 17021187]

Makary CA, Shin J, Kujawa SG, Liberman MC, Merchant SN. Age-related primary cochlear neuronal degeneration in human temporal bones. J Assoc Res Otolaryngol. 2011; 12:711–717. [PubMed: 21748533]

Merchan-Perez A, Liberman MC. Ultrastructural differences among afferent synapses on cochlear hair cells: correlations with spontaneous discharge rate. J Comp Neurol. 1996; 371:208–221. [PubMed: 8835727]

Miura M, Sando I, Hirsch BE, Orita Y. Analysis of spiral ganglion cell populations in children with normal and pathological ears. Ann Otol Rhinol Laryngol. 2002; 111:1059–1065. [PubMed: 12498365]

Moore JK, Simmons DD, Guan Y. The human olivocochlear system: organization and development. Audiol Neurootol. 1999; 4:311–325. [PubMed: 10516391]

Nadol JB Jr. Serial section reconstruction of the neural poles of hair cells in the human organ of Corti. I. Inner hair cells. Laryngoscope. 1983; 93:599–614. [PubMed: 6843252]

Nadol JB Jr. Innervation densities of inner and outer hair cells of the human organ of Corti. Evidence for auditory neural degeneration in a case of Usher's syndrome. ORL J Otorhinolaryngol Relat Spec. 1988a; 50:363–370. [PubMed: 3231458]

Nadol JB Jr. Application of electron microscopy to human otopathology. Ultrastructural findings in neural presbycusis, Meniere's disease and Usher's syndrome. Acta oto-laryngologica. 1988b; 105:411–419. [PubMed: 3400443]

Ohlemiller KK, Lett JM, Gagnon PM. Cellular correlates of age-related endocochlear potential reduction in a mouse model. Hear Res. 2006; 220:10–26. [PubMed: 16901664]

Otte J, Schunknecht HF, Kerr AG. Ganglion cell populations in normal and pathological human cochleae. Implications for cochlear implantation. Laryngoscope. 1978; 88:1231–1246. [PubMed: 672357]

Pauler M, Schuknecht HF, White JA. Atrophy of the stria vascularis as a cause of sensorineural hearing loss. Laryngoscope. 1988; 98:754–759. [PubMed: 3386381]

Robertson D. Functional significance of dendritic swelling after loud sounds in the guinea pig cochlea. Hearing Res. 1983; 9:263–278.

Schaette R, McAlpine D. Tinnitus with a normal audiogram: physiological evidence for hidden hearing loss and computational model. The Journal of neuroscience : the official journal of the Society for Neuroscience. 2011; 31:13452–13457. [PubMed: 21940438]

Schmiedt, RA.; Schulte, BA. Physiologic and histopathologic changes in quiet- and noise-aged gerbil cochleas. In: Dancer, AL.; Henderson, D.; Salvi, RJ.; Hamernik, RP., editors. Noise Induced Hearing Loss. St. Louis: Mosby; 1992. p. 246-258.

Schmitz F, Konigstorfer A, Sudhof TC. RIBEYE, a component of synaptic ribbons: a protein's journey through evolution provides insight into synaptic ribbon function. Neuron. 2000; 28:857–872. [PubMed: 11163272]

Schrott-Fischer A, Kammen-Jolly K, Scholtz A, Rask-Andersen H, Glueckert R, Eybalin M. Efferent neurotransmitters in the human cochlea and vestibule. Acta oto-laryngologica. 2007; 127:13–19. [PubMed: 17364323]

Schuknecht, HF. Pathology of the Ear. 2nd Edition. Baltimore: Lea & Febiger; 1993.

Schuknecht HF, Woellner RC. An experimental and clinical study of deafness from lesions of the cochlear nerve. The Journal of laryngology and otology. 1955; 69:75–97. [PubMed: 14354340]

Sergeyenko Y, Lall K, Liberman MC, Kujawa SG. Age-related cochlear synaptopathy: an early-onset contributor to auditory functional decline. The Journal of neuroscience : the official journal of the Society for Neuroscience. 2013; 33:13686–13694. [PubMed: 23966690]

Seyyedi M, Eddington DK, Nadol JB Jr. Interaural comparison of spiral ganglion cell counts in profound deafness. Hear Res. 2011; 282:56–62. [PubMed: 22008826]

Soucek S, Michaels L, Frohlich A. Evidence for hair cell degeneration as the primary lesion in hearing loss of the elderly. J Otolaryngol. 1986; 15:175–183. [PubMed: 3723657]

Spoendlin H. Innervation patterns in the organ of corti of the cat. Acta oto-laryngologica. 1969; 67:239–254. [PubMed: 5374642]

Spoendlin H. Optic cochleovestibular degenerations in hereditary ataxias. II. Temporal bone pathology in two cases of Friedreich's ataxia with vestibulo-cochlear disorders. Brain. 1974; 97:41–48. [PubMed: 4434170]

Spoendlin H, Schrott A. Analysis of the human auditory nerve. Hear Res. 1989; 43:25–38. [PubMed: 2613564]

Spoendlin H, Schrott A. Quantitative evaluation of the human cochlear nerve. Acta Otolaryngol Suppl. 1990; 470:61–69. discussion 69–70. [PubMed: 2239235]

Spoendlin HH. Innervation densities of the cochlea. Acta Otolaryng. 1972; 73:235–248. [PubMed: 5015157]

Spoendlin HH, Gacek RR. Electron Microscopic Study of the Efferent and Afferent Innervation of the Organ of Corti in the Cat. Ann Otol Rhinol Laryngol. 1963; 72:660–686. [PubMed: 14064974]

Stamataki S, Francis HW, Lehar M, May BJ, Ryugo DK. Synaptic alterations at inner hair cells precede spiral ganglion cell loss in aging C57BL/6J mice. Hear Res. 2006; 221:104–118. [PubMed: 17005343]

Wan G, Gomez-Casati ME, Gigliello AR, Liberman MC, Corfas G. Neurotrophin-3 regulates ribbon synapse density in the cochlea and induces synapse regeneration after acoustic trauma. eLife. 2014:3.

Zilberstein Y, Liberman MC, Corfas G. Inner hair cells are not required for survival of spiral ganglion neurons in the adult cochlea. J Neurosci. 2012; 32:405–410. [PubMed: 22238076]

- Human temporal bones were immunostained and examined by confocal microscopy
- “Normal” ears from 54 to 89 yrs with no history of otologic disease were selected
- Hair cells, synaptic ribbons, cochlear nerve axons and efferent axons were counted
- Results showed cochlear neurodegeneration without hair cell loss in the oldest ears
- Results suggest that primary neural degeneration is important in human presbycusis

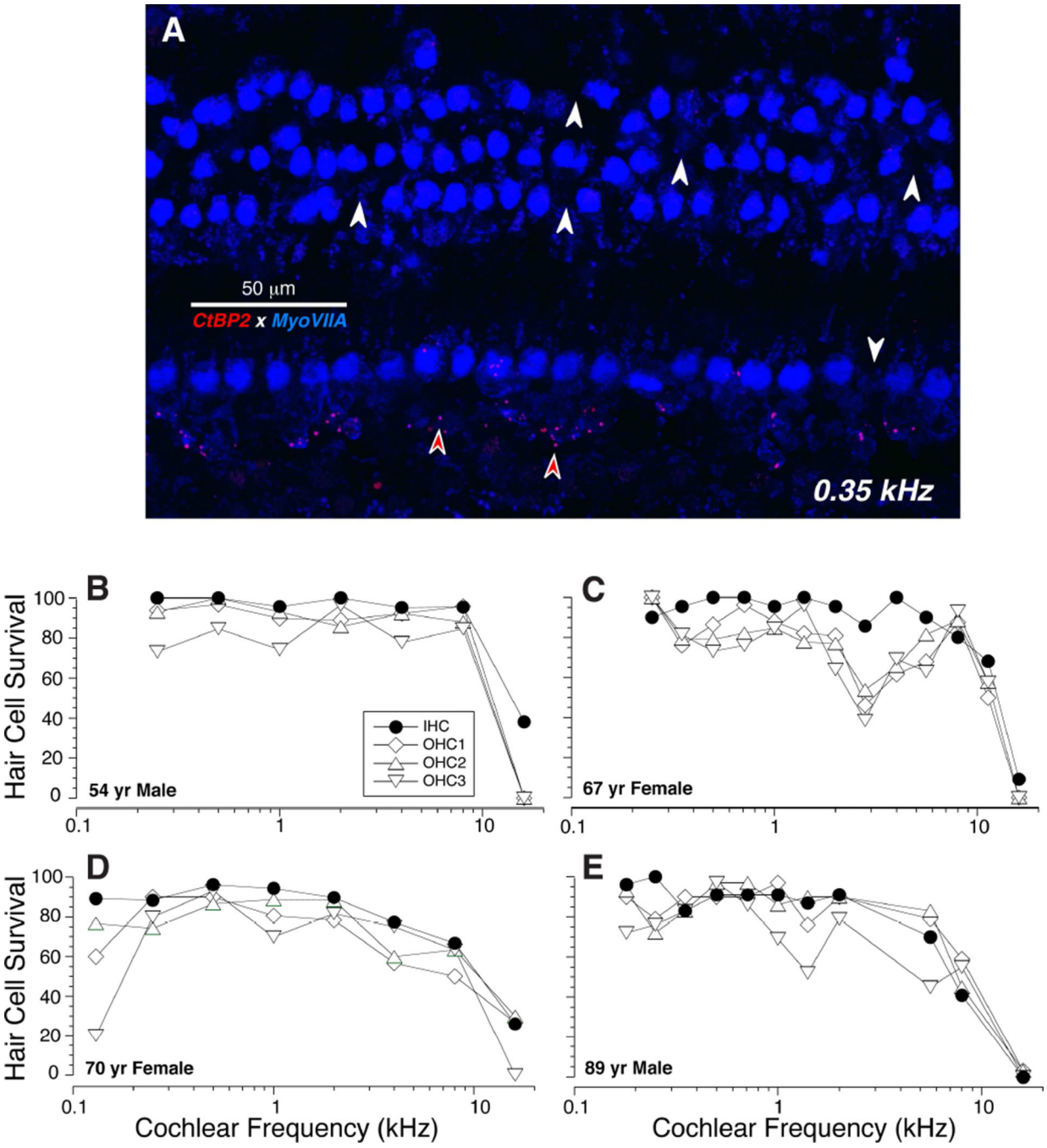

Figure 1.

Cytocochleograms show the limited hair cell loss in the temporal bones studied in this report. **A:** Maximum projection of a confocal z-stack from the 0.35 kHz region in an 89 yr old male, double-immunostained for a hair cell marker (myosin VIIa - blue) and a synaptic ribbon marker (CtBP2 – red). White arrows indicate the locations of some of the missing hair cells. Red arrows indicate some the pre-synaptic ribbons in the inner hair cell area. **B-E:** Cytocochleograms from four human cases computed from images like that in **A**.

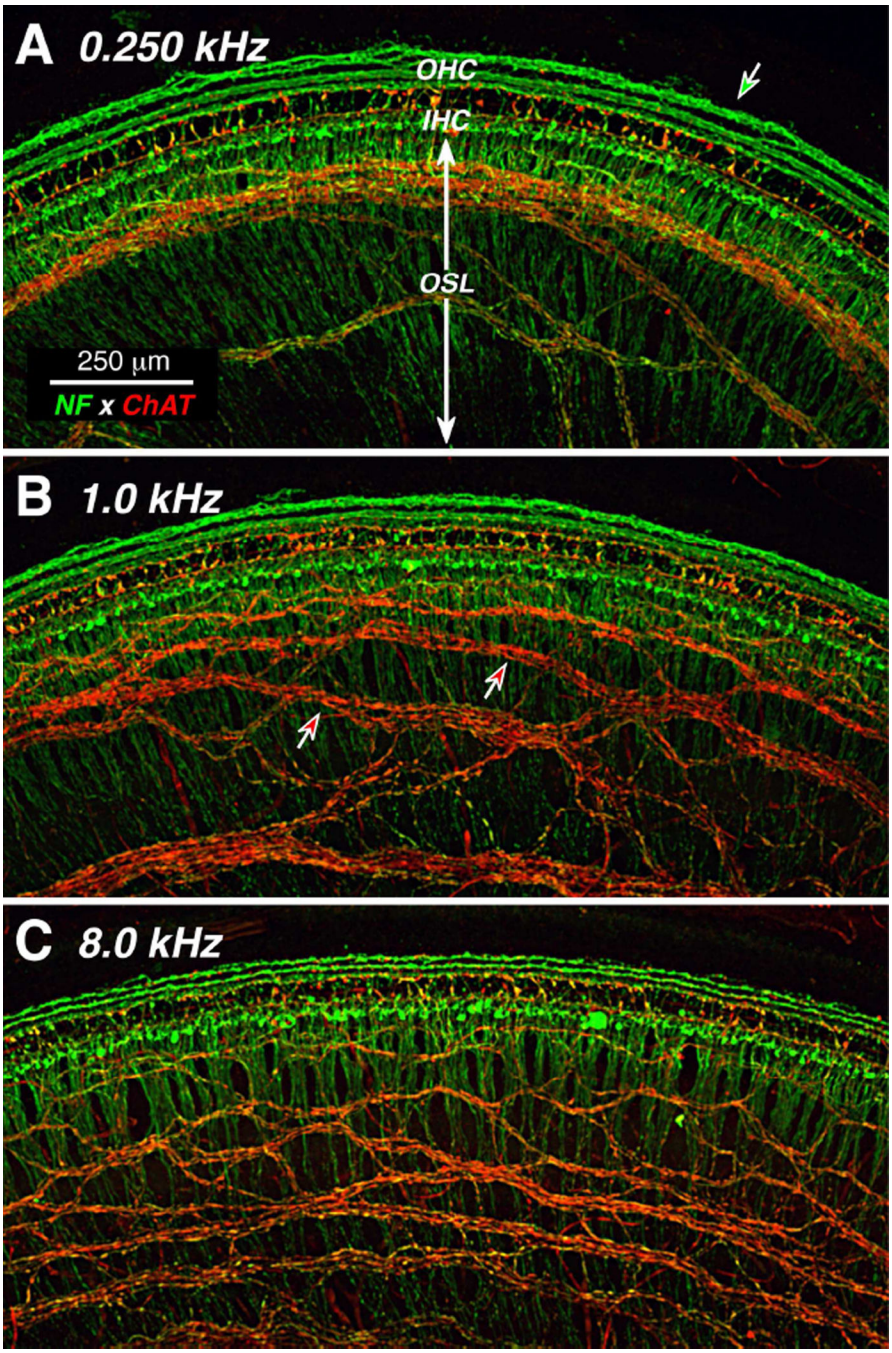

Figure 2.

Double-immunostaining for a general neuronal marker (neurofilament - green) and a cholinergic neuronal marker (choline acetyltransferase [ChAT] - red) distinguishes afferent and efferent fibers. Two types of afferents (green), radial fibers and three rows of outer spiral fibers, are seen in inner and outer hair cell areas, respectively. Cholinergic efferents of the olivocochlear bundle are immunostained by anti-ChAT (red). Images are all from a 54 yr old male. Each is a maximum projection of a confocal z-stack from a different cochlear region, as indicated. Green-filled arrow in **A** points to an anomalous fiber spiraling among

the Hensen cells; green-filled arrow in **B** points to the outermost row of outer spiral fibers; red-filled arrows in **C** point to fascicles of spiraling efferent fibers. Scale in **A** applies to all panels.

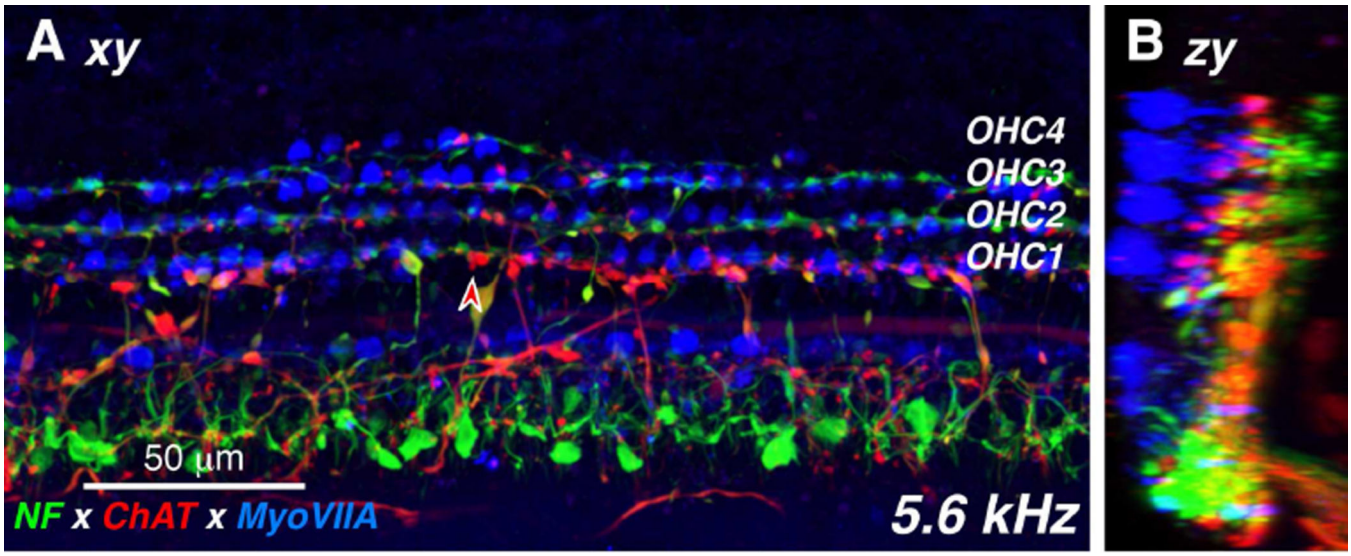

Figure 3.

The distribution of cholinergic efferent terminals under the inner and outer hair cells is seen in these high-power views of the organ of Corti, triple-immunostained for a general neuronal marker (neurofilament – green), a cholinergic neuronal marker (choline acetyltransferase – red) and a hair cell marker (myosin VIIa – blue). The image in **A** is a maximum projection from confocal z-stack through the 5.6 kHz region of a 54 yr old male. The image in **B** is a zy re-projection of the same z-stack. The red-filled arrowhead in **A** points to one ChAT-positive efferent terminal on a first-row outer hair cell.

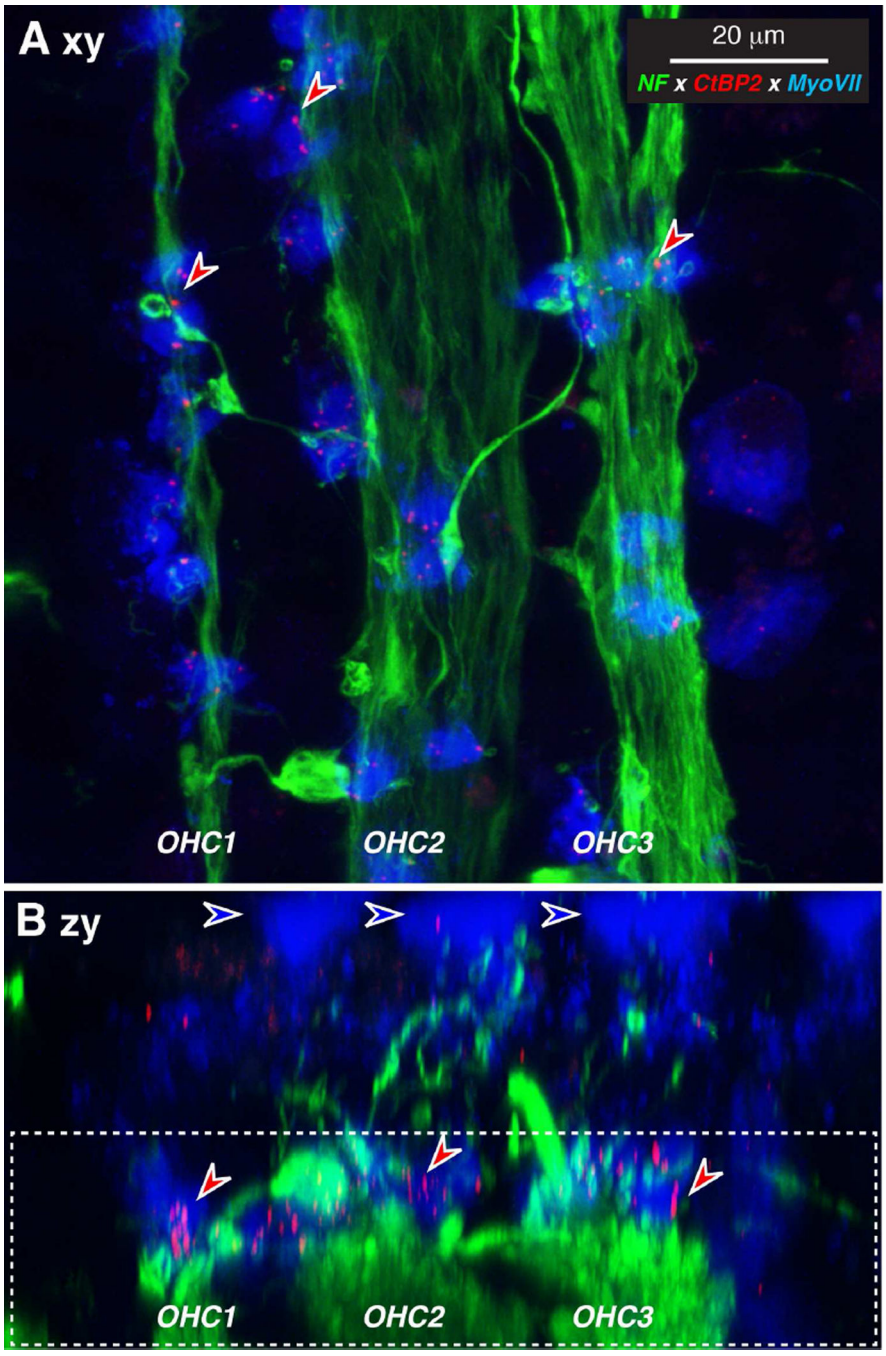

Figure 4.

OHC synaptic ribbons can be seen after immunostaining for a ribbon protein (CtBP2 – red), a neuronal marker (neurofilament – green) and a hair cell marker (myosin VIIa – blue). **A:** Maximum projection of a confocal z-stack from the 1.0 kHz region of a 70 yr old female, displayed in the acquisition plane (xy). **B:** Re-projection in the zy plane shows that the ribbons (e.g. at the red arrows) are within the basal ends of the OHCs. Blue-fill arrows indicate the cuticular plates. Dashed box in **B** indicates the portion of the z-stack projected in **A**. Scale bar in **A** applies to both panels.

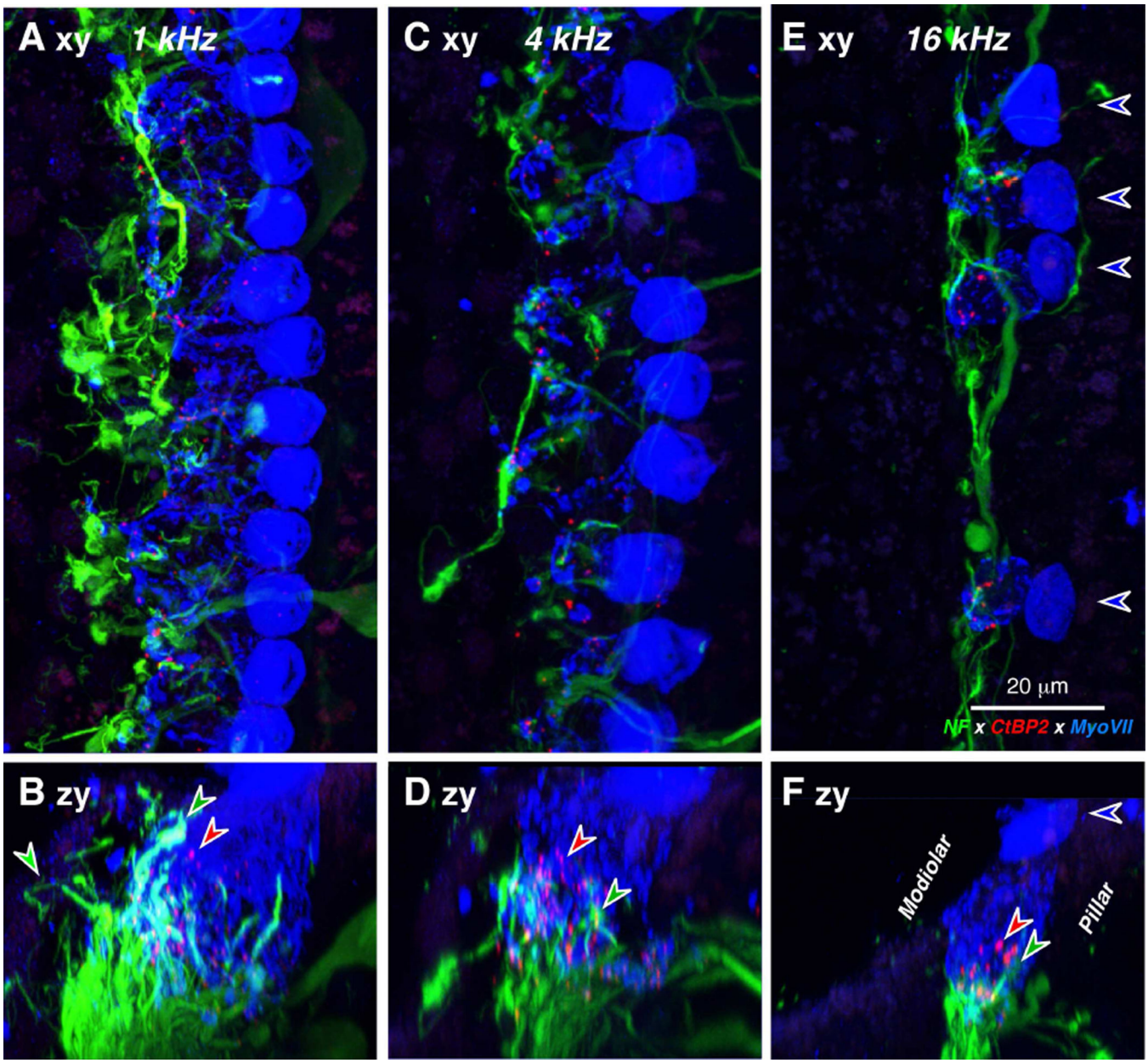

Figure 5.

IHC synaptic ribbons can be seen after immunostaining as in Figure 4. **A,C,E:** Maximum projections of confocal z-stacks from the 1.0, 4.0 and 16.0 kHz regions, respectively of a 67 yr old female, displayed in the acquisition plane (xy). Blue-fill arrows indicate the cuticular plates of 4 remaining IHCs and point away from the OHCs. **B,D,F:** The same three z-stacks re-projected in the zy plane, to show that the ribbons (e.g. at the red arrows) are within the basal ends of the IHCs, where the cochlear nerve fibers terminate (e.g. green arrows). Scale bar in **E** applies to all panels.

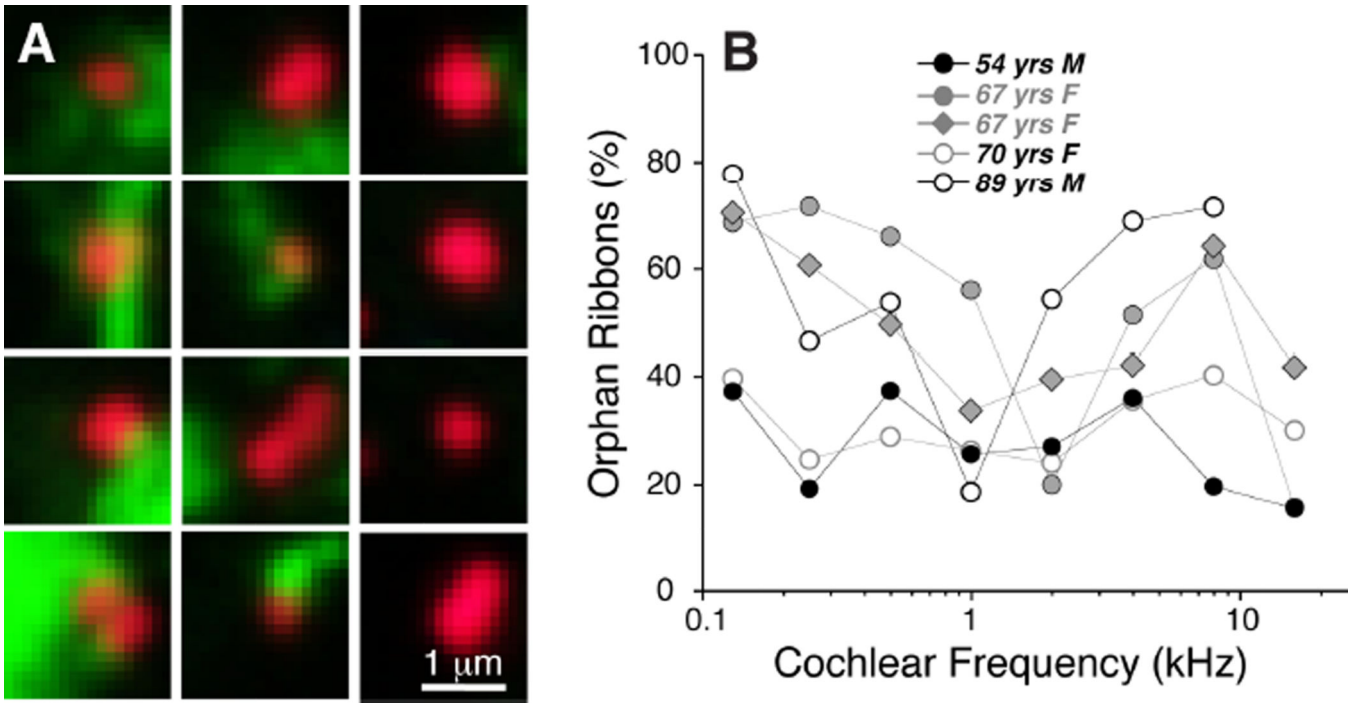

Figure 6.

Analysis of orphan ribbons in the IHC area. **A:** Thumbnail re-projections of the voxel space immediately surrounding 12 selected synaptic ribbons from the z-stack shown in Fig. 5A. Some ribbons are clearly juxtaposed to nerve terminals (left two columns) while others are not (right column). Only the red (anti-CtBP2) and green (anti-neurofilament) channels are shown for clarity. **B:** Percentage of orphan ribbons, i.e. those not closely juxtaposed to post-synaptic terminals, as assessed by evaluating thumbnail arrays such as those illustrated in **A**, for each of the five completely reconstructed ears in the present study.

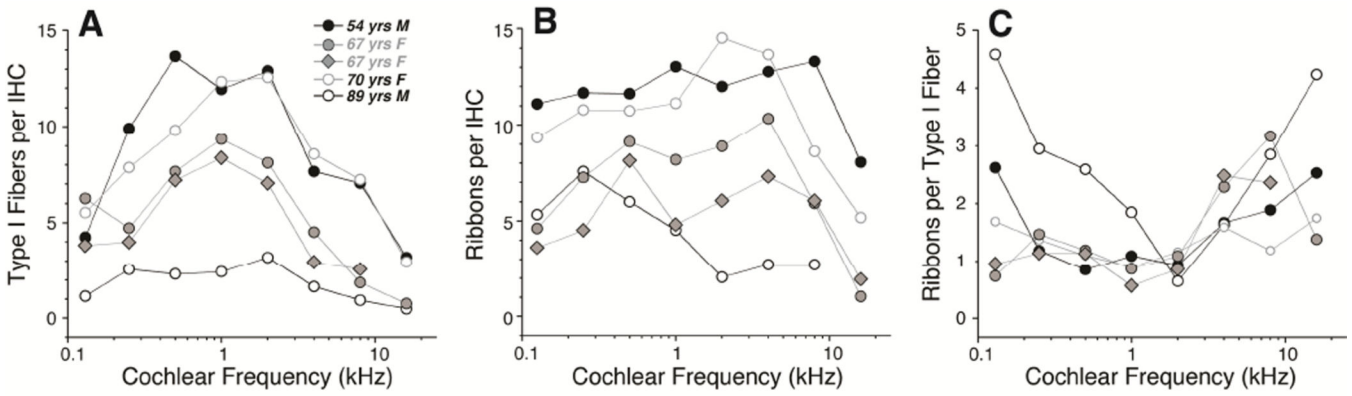

Figure 7.

Quantification of synaptic and neural elements in the five reconstructed cases from the present study suggests age-related synaptopathy in the IHC area. **A:** Counts of the peripheral axons of type-I cochlear nerve fibers as a function of cochlear location. Data are extracted from xz slices through the OSL as illustrated in Figure 8 and described further in Methods. **B:** Counts of synaptic ribbons per IHC as a function of cochlear location. Data are extracted from confocal z-stacks like those shown in Figure 5 and described further in Methods **C:** Counts of ribbons per type-I axon are computed by dividing the data in **B** by the data in **A**.

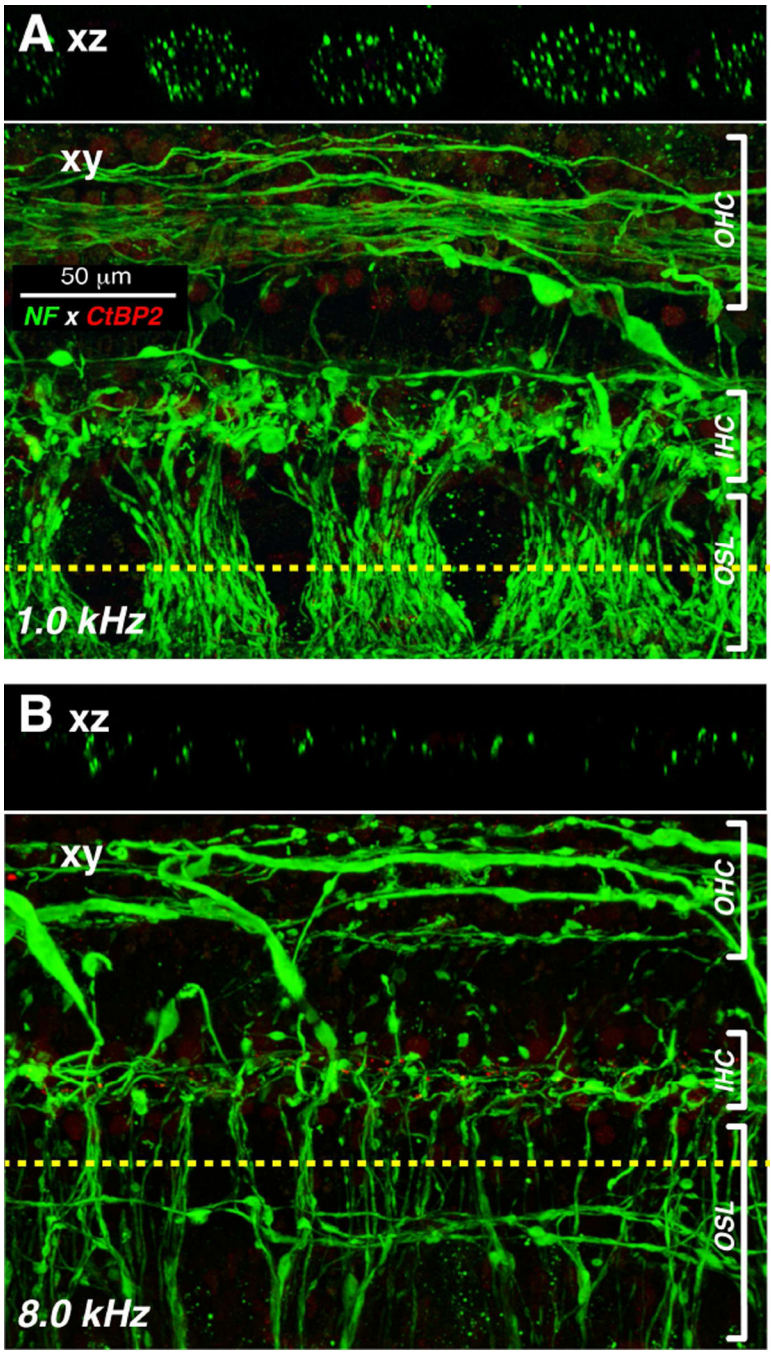

Figure 8.

Basal-turn degeneration of cochlear nerve peripheral axons is seen in confocal image stacks through the osseous spiral lamina and organ of Corti from the 1 and 8 kHz region of a 67 yr-old female. **A-B**: Each pair of images shows, at a different cochlear location, the maximum projection (xy) of a confocal z-stack immunostained for neurofilament (green), along with an orthogonal “slice” through the image stack (xz plane) at the position indicated by the dashed yellow line.

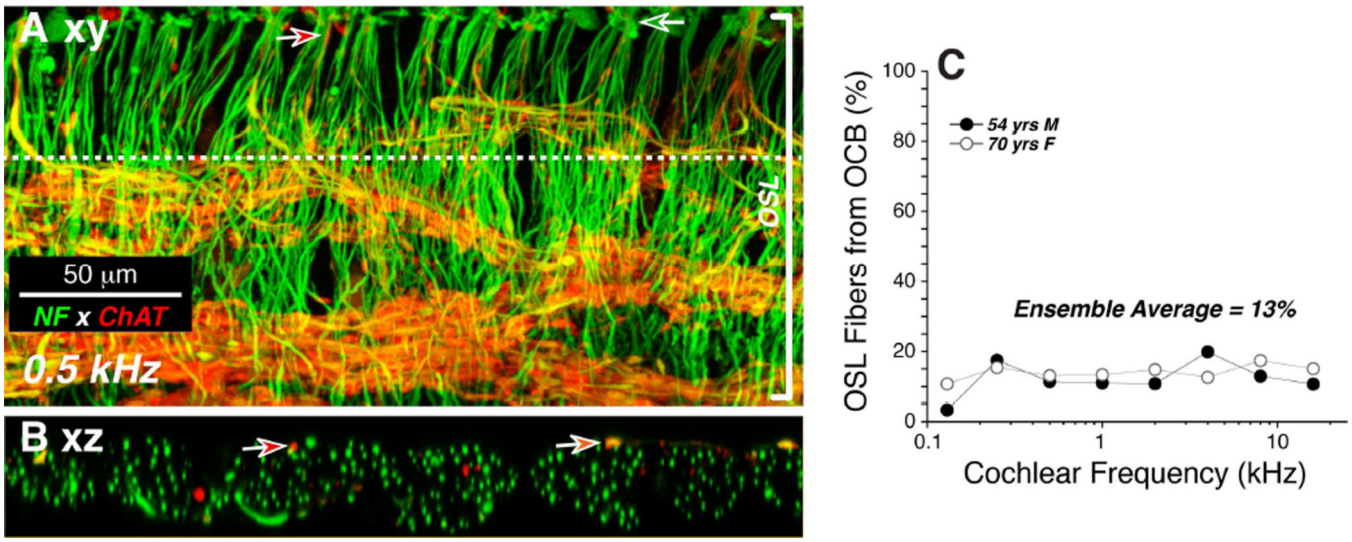

Figure 9.

The ratio of afferent to efferent fibers in the osseous spiral lamina (OSL) can be estimated by comparing the total axonal counts (neurofilament, green) to counts of cholinergic axons (choline acetyltransferase, red). **A:** Maximum projection of a z-stack through the osseous spiral lamina (OSL) in the 0.5 kHz region of a 54 yr old male. Dashed line indicates the position of the re-projected "slice" shown in **B**. Green arrow shows one fascicle entering the habenula. Red arrow shows one efferent fiber near the habenula. **B:** Digital slice through the z-stack at the position indicated by the dashed line in **A**. Red arrows show two efferent fibers among the numerous afferent (ChAT-negative) fibers. **C:** Percentage of OSL axons that are ChAT-positive, and therefore from the olivocochlear bundle (OCB). Data are from the two cases with the OSL axonal counts. Ensemble average (13%) is for all frequency regions from both cases.

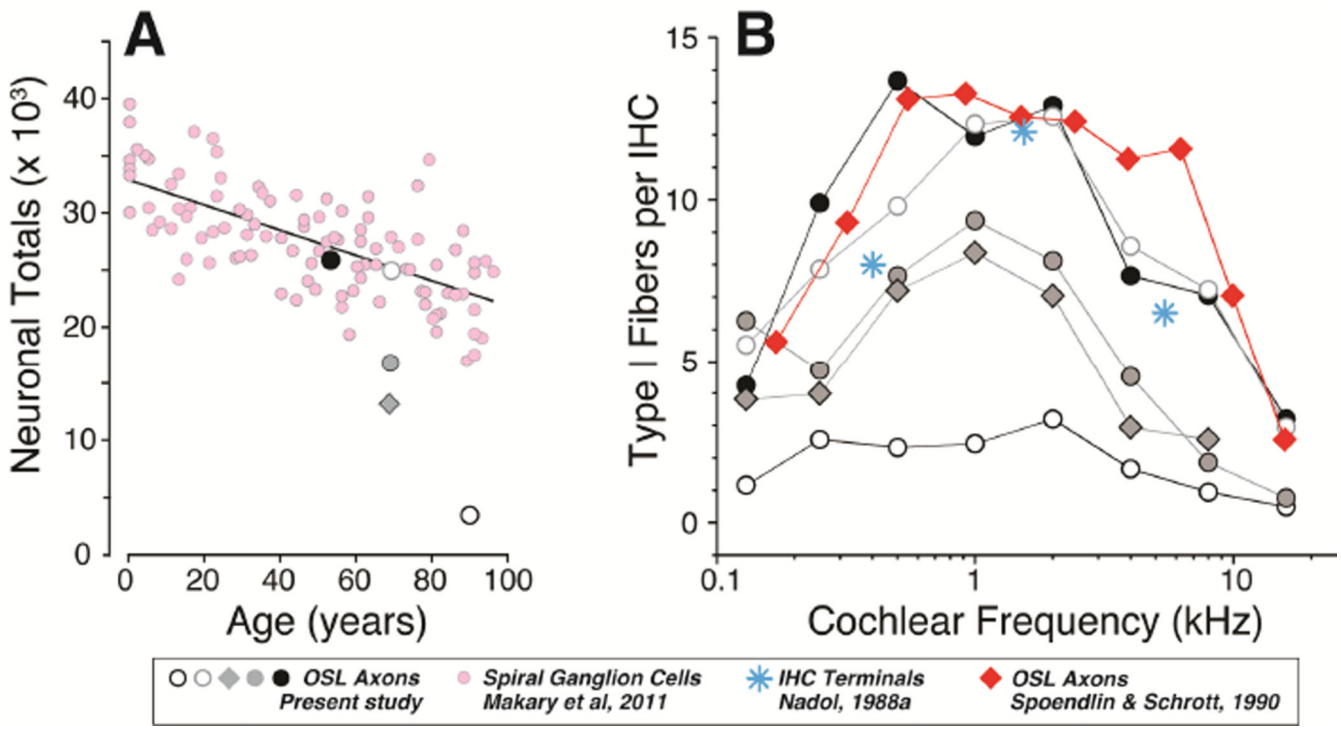

Figure 10.

Comparisons between present data and prior human studies of spiral ganglion counts (**A**) or peripheral axon and synaptic counts (**B**). **A**: Peripheral axon counts (from Fig. 7A) are used to estimate the total number of type-I ganglion cells in each of the five cases (see text for further explanation) and then compared to counts of spiral ganglion cells in an age-graded series of temporal bones from a previous study [pink, (Makary et al., 2011)]. **B**: Counts of type-I peripheral axons (from Fig. 7A) are compared to similar counts from a prior light-microscopic study [red, (Spoendlin et al., 1990)], and to counts of terminals per IHC from an electron microscopic study of a 64 yr old male [blue, (Nadol, 1988a)]. The peripheral axon counts from a prior study are averages of two ears from a 7-yr old, extracted from their Figure 6 (Spoendlin and Schrott, 1990) and then converted from fibers/mm to fibers/IHC using a mean value of 10.6 mm on-center spacing for IHCs extracted from confocal images such as those in Figure 1A. Symbol key applies to both panels.